2010 TOPCO 崇越論文大賞

論文題目

InGaN-based Light-Emitting Solar Cell (LECS) with Inverted Pyramid Structures Through Laser Scribing and Chemical Etching Processes

報名編號： SC0014

Abstract

The InGaN-based light-emitting diodes (LEDs) with a roughened patterned backside on the N-ace GaN surface were fabricated through a crystallographic etching process to increase light extraction efficiency. After laser decomposition, laser scribing, and a lateral crystallographic wet etching process at the GaN/Al_2O_3 interface, stable crystallographic etching planes were formed as the GaN $\{10\overline{1}\overline{1}\}$ planes that included an angle with the top GaN (0001) plane measured at 58^o. The GaN buffer layer acted as the sacrificial layer for the laser decomposition process and the lateral wet etching process with a 26 μm/min etching rate. The LED with the inverted pyramidal N-face GaN surface close to the GaN/Al_2O_3 interface has a larger light scattering process than the conventional LED. The light output power of the LED with the backside roughened surface had a 47% enhancement when measured in LED chip form.

Then, this technique was used on the InGaN-based LED structure grown on a patterned-sapphire substrate (PS-LED) to form the inverted pyramid structures. The light output power of the BRPS-LED with the backside roughened surface had a 21.4% enhancement compared to a conventional PS-LED in chip form. The larger divergent angle of BRPS-LED could be caused by light-scattering process from the inverted pyramidal-shaped structures on the roughened patterned backside surface at the GaN/Al_2O_3 interface.

The InGaN light-emitting solar cell devices were fabricated through a laser decomposition stripe-line patterns by varying the stripe-line spacing width. By reducing the spacing-width from 40μm to 10μm, the short-circuit current density (Jsc) value of the RB-LESC structures were increased from $0.83 mA/cm^2$ to $1.23\ mA/cm^2$ by increasing the backside roughened area at the mesa region. The peak EQE value and Jsc were increased by increasing the laser-treated roughened area ratio. The highest peak EQE value and Jsc were measured at 0.75 (at 373.4 nm) and $1.23 mA/cm^2$ for the BR-LESC structure with a 10μm spacing width that had a 66% backside roughened ratio on mesa region.

Chapter 1 Introduction

1-1 The Evolution of the Light

Since 1879 the incandescent lamps were invented, and fluorescent lights, tungsten halogen lamps, sodium lamps and mercury lamp develop subsequently. With the evolution of lighting technology, the solid lighting was improved from the heat radiation and gas discharge light to the solid field light.

The past 10 years have seen significant development of GaN-based light-emitting diodes (LEDs). At present, GaN-based LEDs are being marketed and used for a variety of applications, including traffic signals, full-color displays, back lighting in liquid-crystal displays, and white LEDs. Recently, high-efficiency white LEDs have caught much attention because the replacement of fluorescent lamps will be realistic in the future. The blue LED is combined with yellow fluorescent powder that blue LED will activate the yellow fluorescent powder to illuminate the yellow-light, and both of them mix to form the white-light. Although market already have the different colors LEDs including red, orange, yellow, and green, the source of displays must have high efficiency ,high power blue-light and green-light. If GaN, InGaN, AlInGaN as LEDs materials can be served as LED materials, the high power blue-light and green-light can be investigated. Combined with the complete technology of red LEDs achieve the requirement of full-color displays. In the future, the high power LEDs will replace the traditional bulb-based traffic signals and improve the sharpness, and up to energy saving.

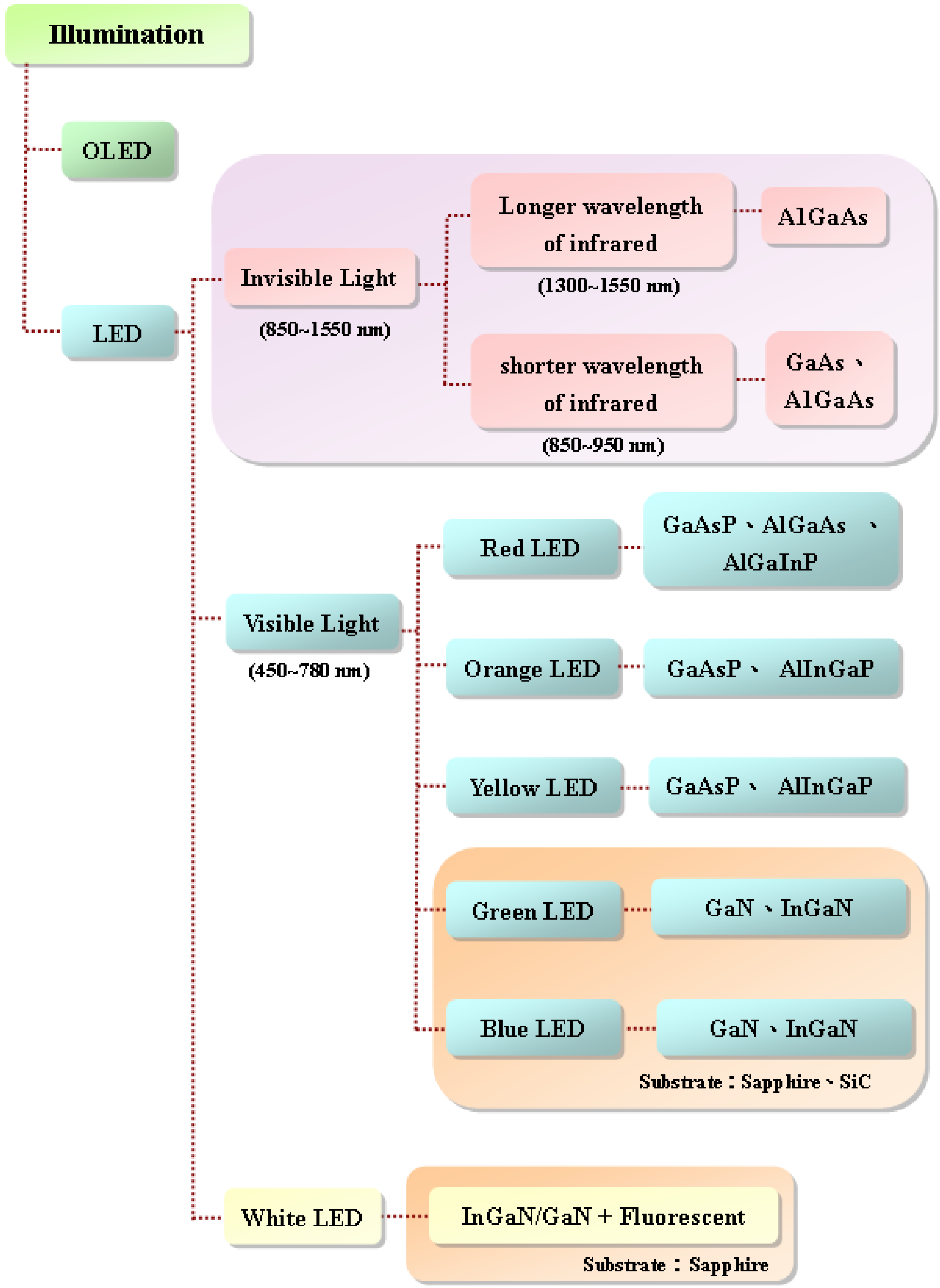

Fig. 1-1 The color classification diagram of light-emitting diode.

1-2 Background of Light-Emitting Diodes

Ш-nitride materials based on GaN (bandgap is 3.4eV), InN (bandgap is 0.7eV) and AlN (bandgap is 6.2eV) have been extensively investigated because of their potential for use in light-emitting diodes (LEDs), which operate in the blue and ultraviolet (UV) wavelength regions [1-3], and GaN has excellent electronic, optical, and thermal properties. These LEDs have already been used in a variety of applications, such as outdoor full-color displays, traffic lights, indicators, indoor illuminations, and liquid crystal display (LCD) backlights [4]. This widespread application makes it desirable to increase the internal quantum efficiency (η_{int}) and light extraction efficiency ($\eta_{extraction}$) of LEDs.

Gallium nitride materials have attracted considerable interest in the development of optoelectronic devices like light-emitting diodes (LEDs) and laser diodes. However, bright blue LEDs require an increase in their internal and external quantum efficiencies. The lower external quantum efficiency of the InGaN-based LEDs is due to a larger refractive index difference between the GaN layer and the surrounding air (Δn~1.5). Bottom patterned Al_2O_3 substrates [5], top p-type GaN:Mg rough surface processes [6,7], the formation of photonic crystal structures [8,9], periodic deflector embedded structures [10], and selective oxidization on the mesa sidewall [11] through a photoelectrochemical (PEC) wet oxidation process have been used to increase light-extraction efficiency in InGaN-based LEDs on Al_2O_3 substrates. Fujii *et al.* [12] reported that a laser-lift-off technique followed by an anisotropic etching process to roughen the surface - an n-side-up GaN-based LED with a hexagonal ‘‘conelike’’ surface - has been fabricated to increase extraction efficiency. Kim *et al.* [13] have reported that GaN-based light-emitting diodes with peripheral microhole arrays (PMA-LEDs) have been grown and fabricated on SiO_2 hexagonal pattern masks using a selective metal–organic chemical vapor deposition, and the light-output intensity of the PMA-LED was 30% higher than that of the conventional LEDs. Stocker *et al.* [14] reported that crystallographic wet chemical etchings of the n-GaN have (0001), $\{10\bar{1}0\}$, $\{10\overline{11}\}$, $\{10\overline{12}\}$ and $\{10\overline{13}\}$ stable planes.

1-3 Ⅲ-Ⅴ Semiconductor

Ⅲ-Ⅴ Semiconductor can fabricate blue、green and ultraviolet (UV) LEDs because of it have direct bandgap、wide bandgap、the property of resistant-radiation、good thermal diffusion and strong chemical bonding. In Fig. 1-2, it obtains the bandgap of the AlN、GaN and InN are 6.2eV、3.4eV and 0.7eV, respectively. If we change the ratio of the two linear of Al、Ga、N or In、Ga、N, we can obtain different wavelength in LEDs and it obtain not only the visible、UV wavelength but also infrared range. [1,3,15]

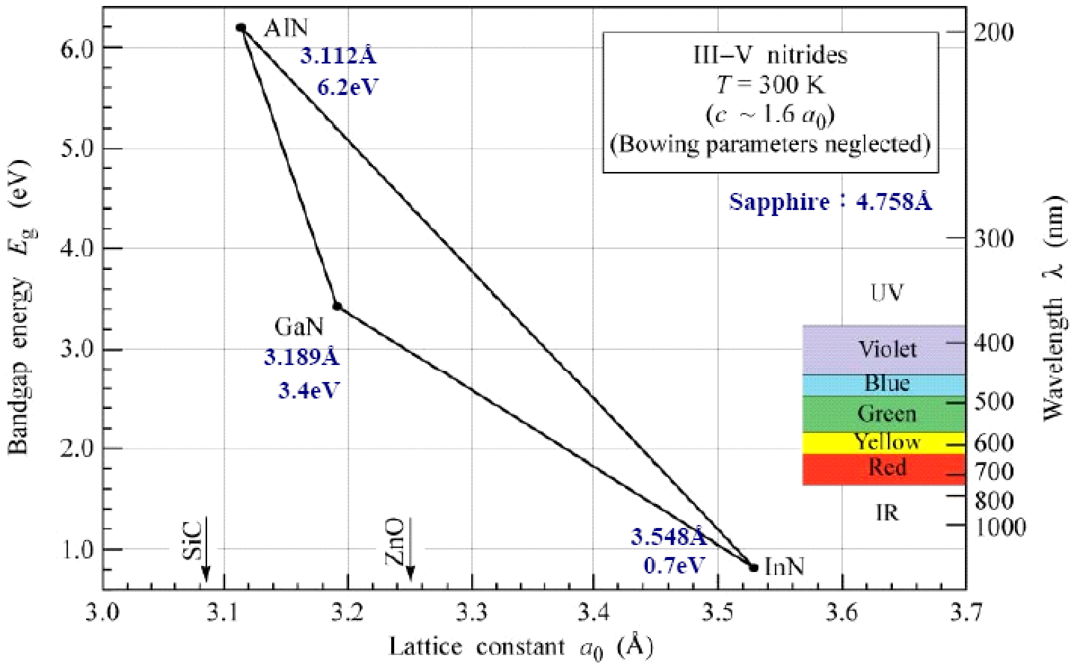

Fig. 1-2 The curve of the bandgap and lattice constant of Ⅲ-Ⅴ Semiconductor.

Chapter 2 Experiment

2-1 Specimen Preparation Process

InGaN-based LED structures were grown on a two-sided polished optical-grade C-face (0001) 2”-diameter sapphire substrate by using a metalorganic chemical vapor deposition (MOCVD) system. These LED structures consisted of a 30nm-thick GaN buffer layer, a 1μm-thick unintentionally doped GaN layer, a 3.5μm-thick n-type GaN layer, 10 pairs of the InGaN/GaN multiple quantum wells (MQWs) active layers, and a 0.4μm-thick magnesium-doped p-type GaN layer. The active layers consisted of a 30Å-thick InGaN-well layer and a 70Å-thick GaN-barrier layer for the InGaN/GaN MQW LED structure. We cleaved a 2” LED wafer into two half-wafers to prepare for this experiment, with a mesa region of 533×216 μm^2.

Next, the mesa region was defined through the inductively coupled plasma (ICP) etcher using Cl_2 gas. A 240nm-thick indium-tin-oxide layer (ITO) was deposited on the mesa region as a transparent contact layer (TCL). The Cr/Au metal layers were deposited as n-type and p-type contact pads as shown in Fig. 2-2(a) and (b). The LED device that was fabricated through this process flow without a laser decomposition process was defined as a standard LED (ST-LED). The LED device that was fabricated by adding the laser decomposition process, the laser scribing process, and the crystallographic wet etching process was then defined as a roughened patterned backside LED (RPB-LED). The diagram of laser scribing equipments are shown in Fig 2-3 (a) and (b).

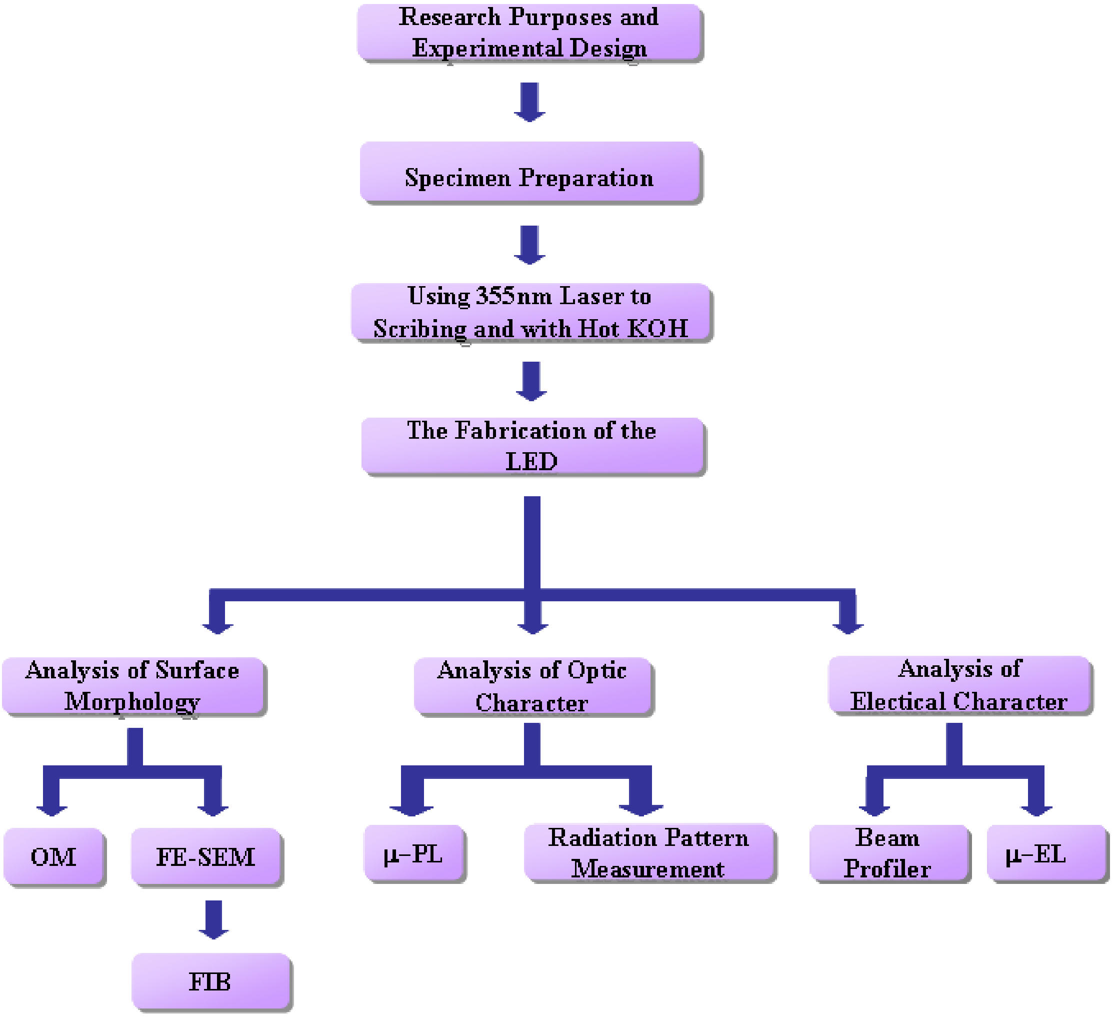

Fig. 2-1 Experimental design diagram

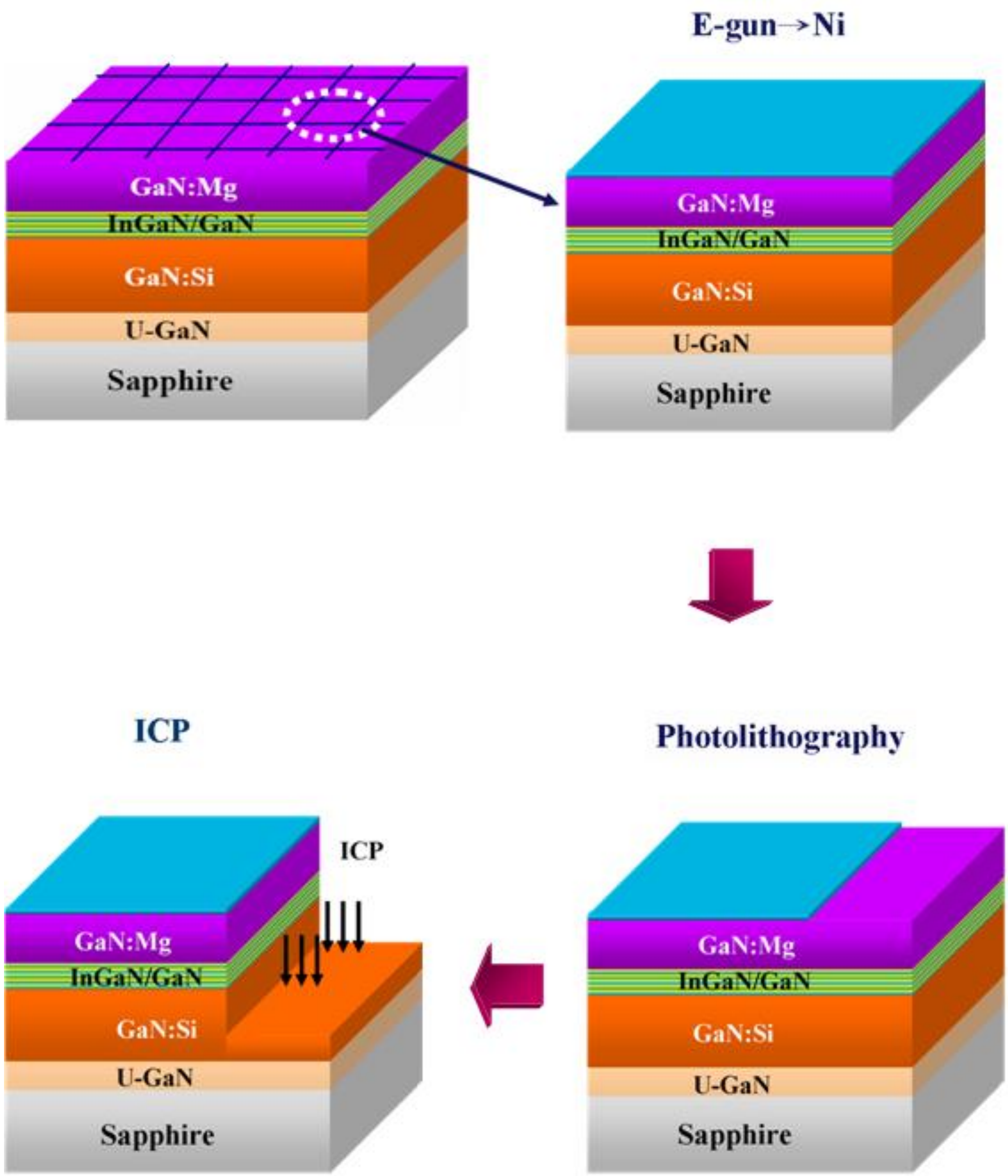

Fig. 2-2(a) Schematic diagram of light-emitting diodes (LEDs)

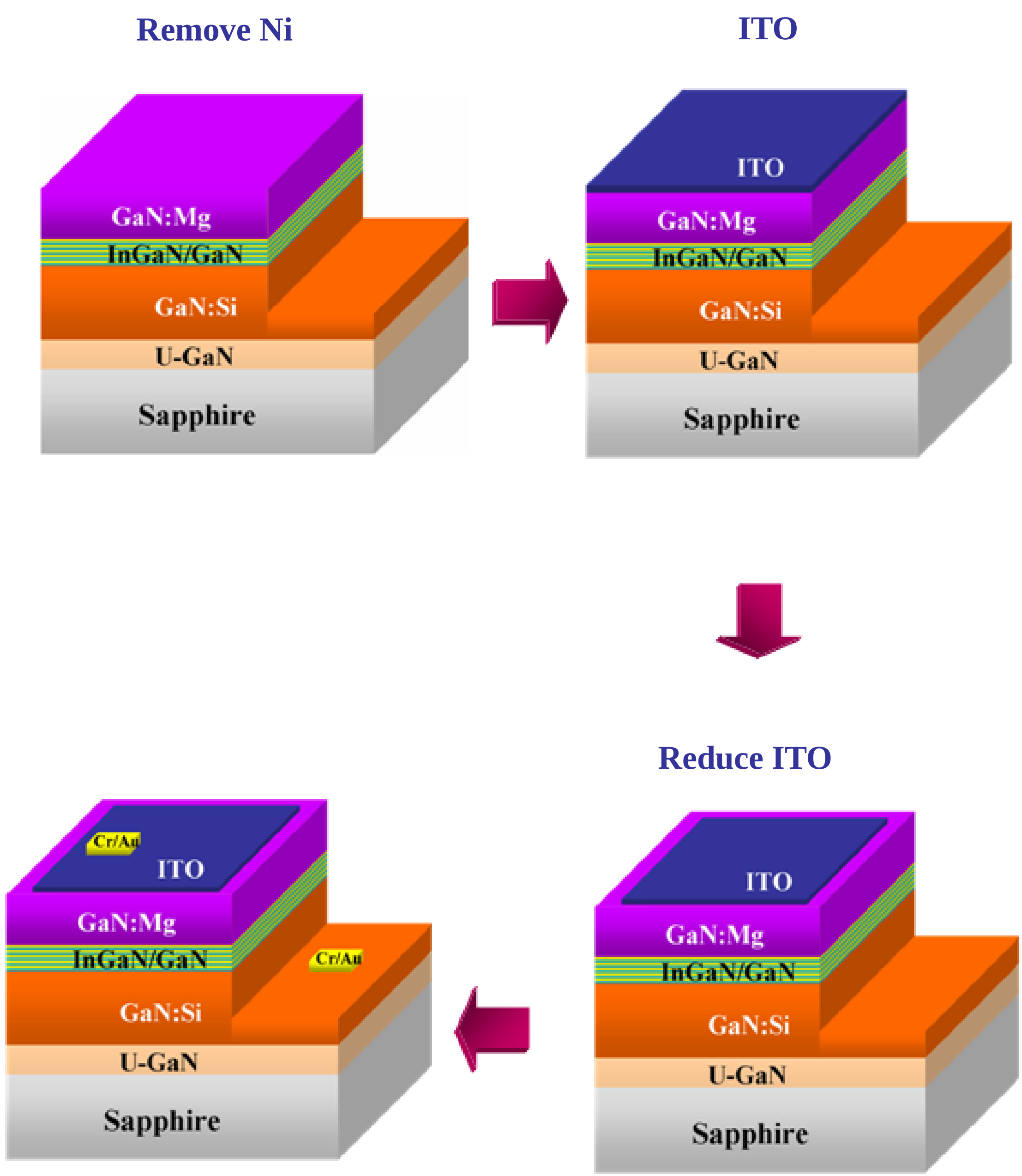

Fig. 2-2(b) Schematic diagram of light-emitting diodes (LEDs)

(a)

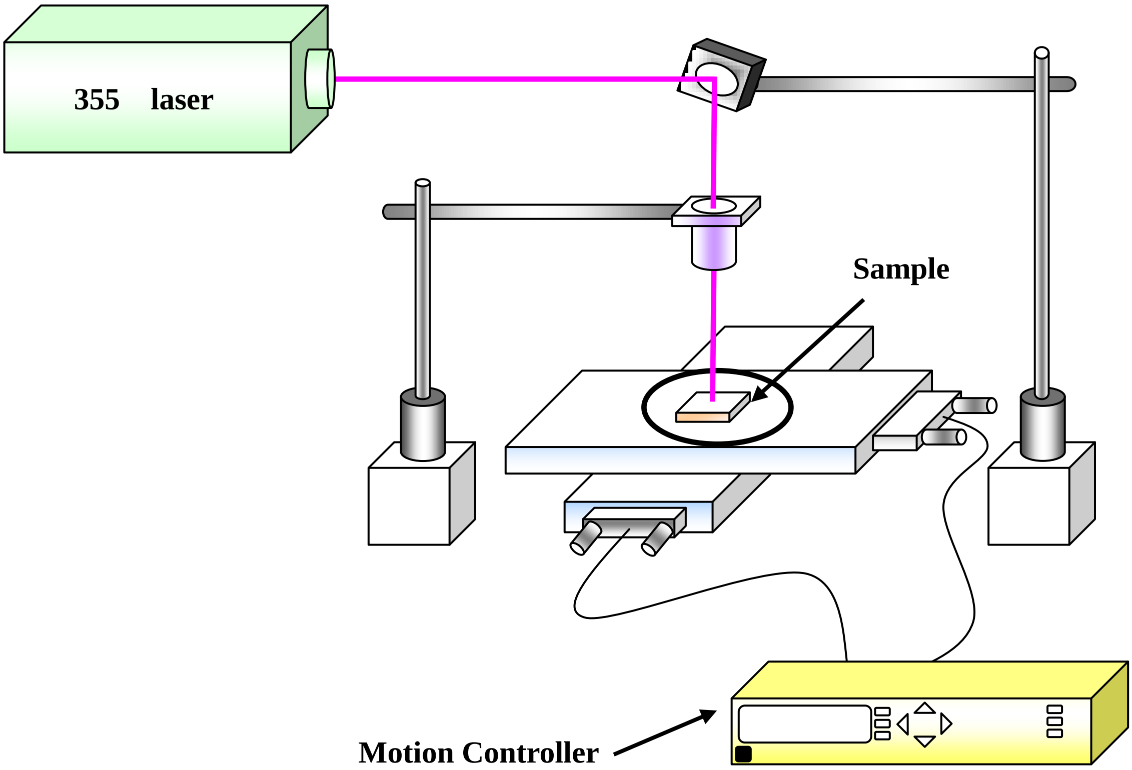

(b)

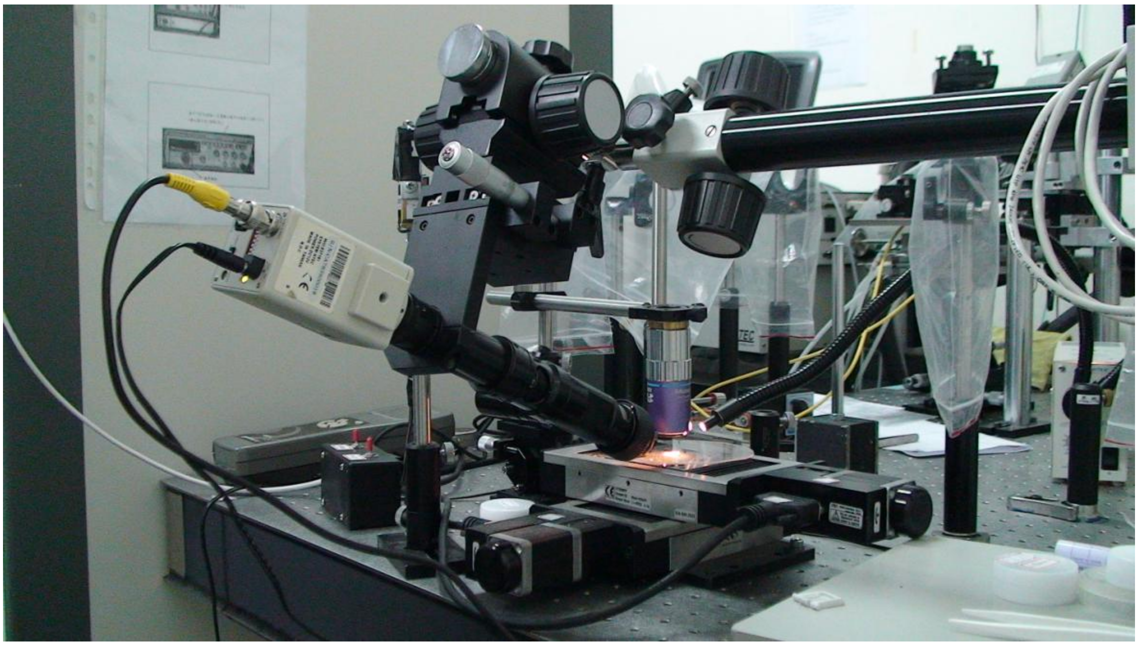

Fig. 2-3 The diagram of (a) laser scribing equipments and (b) the experimental picture.

2-2 The fabrication of the RPB-LED structure

Using a triple frequency ultraviolet Nd:YVO_4 (355nm) laser for the backside GaN melting and decomposition process. The grid pattern, with a 20µm-width and a 50µm-spacing, were fabricated through a backside laser decomposition process at the GaN/sapphire interface. Then, the same as above, using a triple frequency ultraviolet Nd:YVO_4 (355nm) laser for the front-side laser scribing process on n-GaN. Eventually, half of the LED wafer was immersed in a hot HCl solution for 1-minute and a hot KOH solution (KOH, 80^{o}C) for a 5-minute lateral crystallographic wet etching process that occurred at the laser treated grid-line pattern regions. The wet etching process consisted of a selective lateral etching process on a GaN buffer layer and a bottom-up N-face crystallographic etching process to form the pyramidal N-face GaN structure close to the GaN/sapphire interface. The schematic of the RPB-LED structure was shown in Fig. 2-4.

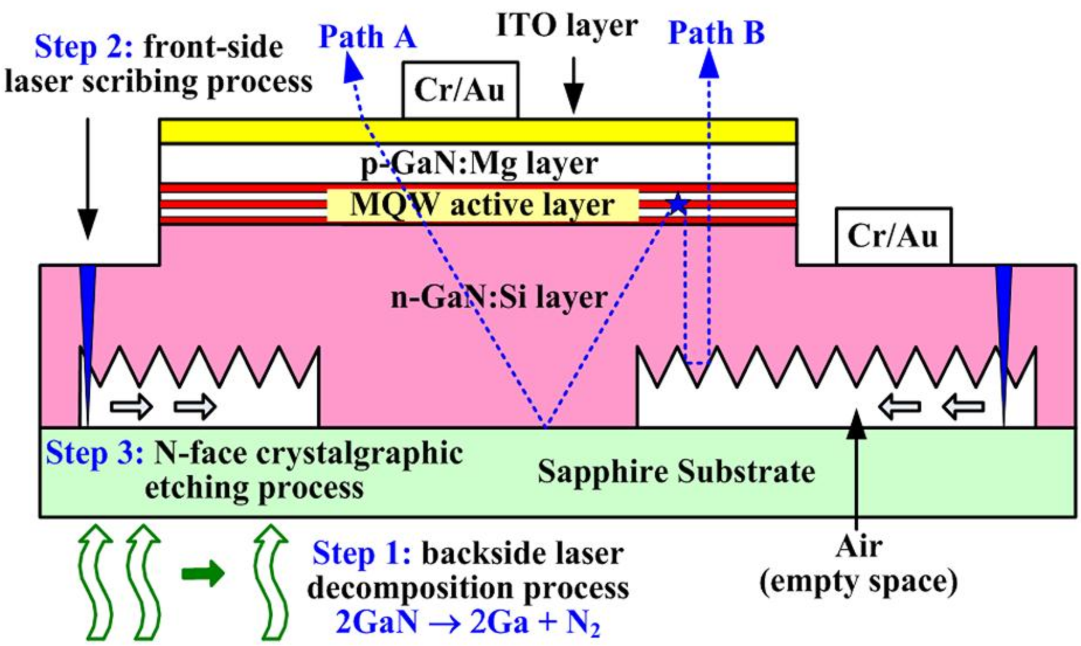

Fig. 2-4 The schematic of the RPB-LED structure

2-3 The fabrication of the BRPS-LED structure

The LED chips were treated by using a triple frequency ultraviolet Nd:YVO_4 (355nm) laser for the front-side laser isolation process and the backside GaN melting process. During the laser melting process at GaN buffer layer, the laser spot was focus on the bottom GaN/patterned-sapphire interface. The striped patterns, with a 20μm-width and a 20μm-spacing, were fabricated through a backside laser melting process on GaN buffer layer at the GaN/sapphire interface. The GaN buffer layer decomposed as Ga metal and N_2 gas through the laser decomposition process. The dimension of the LED chip was 570×240 μm^2 in size defined by the laser scribing process. Half of the LED wafer was immersed in a hot KOH solution (KOH, 80^oC) for a 15-minute lateral crystallographic wet etching process that occurred at the laser treated grid-line pattern regions. The wet etching process consisted of a selective lateral etching process on a GaN buffer layer and a bottom-up N-face crystallographic etching process to form the pyramidal N-face GaN structure close to the GaN/sapphire interface. The LED device that was fabricated through this process flow without a laser decomposed process was defined as a patterned-sapphire LED (PS-LED). The LED device that was fabricated by adding the laser scribing process, the laser melting process, and the crystallographic wet etching process was then defined as a roughened-backside of a patterned-sapphire LED (RBPS-LED). The schematic of the BRPS-LED structure was shown in Fig. 2-5.

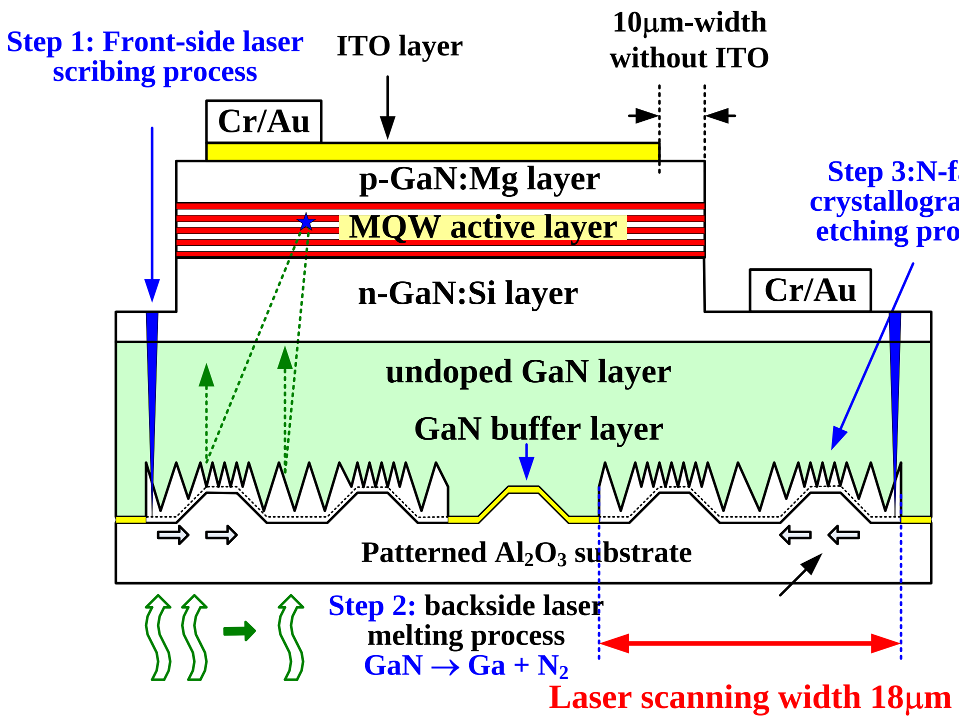

Fig. 2-5 The schematic of the BRPS-LED structure

2-4 Characteristic Methods

2-4-1 The Optical Microscopy (OM)

The optical microscopy(OM) was observed that after and before the laser scribing line width and color change. By objective with 10X, and connected another objective 5X、10X、20X、50X and 100X to microscopic observation, that could quickly find out the variation of the laser scribing line width and color with the morphology of the front-side and back-side light. The preliminary observations was very important to carried out experiments for the follow-up.

2-4-2 The Cold Field Emission Scanning Electron microscopy (FE-SEM)

Due to the advantage of easy handing of preparing a sample, scanning electron microscopy (SEM) has become a widely tool in characterizing sample surface morphology and cross-sectional configuration. The SEM sample is typically coated with a thin Pt layer to increase the electric conductivity of the material so that accumulation of electrons on the sample surface can be minimized during the SEM operation. In this study, the JEOL JSM-6700F cold cathode field-emission SEM was investigated the material surface and structure. The acceleration voltage is from 0.5KV to 30KV, and the magnification is from 50X to 1.5millionX. The resolution is 1nm for 15KV acceleration voltage and 2.2nm for 1KV acceleration voltage.

2-4-3 Micro-Photoluminescence Spectroscopy (μ-PL)

Photoluminescence spectroscopy is a contactless, nondestructive used method of analysis technique for optical properties of Ⅲ-Ⅴ semiconductor materials. The quantum mechanics can be described as an excitation to a higher energy state and then a return to a lower energy state accompanied by the emission of a photon. There occurs electron-hole pairs, and those electron-hole pairs may recombine. There are two ways to recombine the electron-hole pairs. One is non-radiative recombination paths, another is radiative recombination paths. Principle of the PL technique is based on the three distinct processes is based on the three distinct processes occur resulting in the light emission in the samples. (1) absorption of exciting light having energy higher than the bandgap of the material and thus creation of electron-hole pairs, (2) partial radiativere combination of these electron-hole pairs, and (3) escape of this radiation from the optical-pumped material. In general, there are various fundamental radiative transitions in semiconductor, including donor to hole transition, electron to acceptor transition, donor to acceptor transition, band to band tramsition and free exciton transition. In this study, the μ-PL system setup uses the 325nm excitation of a 45mW He-Cd laser. The system includes mirrors, filter, collection lens, dichroic mirror, and microscope objective lens in the optic axis as shown in Fig. 2-6. The dichroic mirror is made by UV fused silica used to selectively passed visible light while reflecting 325nm laser. The microscope objective lens (15X and NA=0.32) is formed a focused spot on the sample surface, and the diameter of focused spot size is 10μm. This PL signal is collected using confocal microscope system and transmitted by multi-mode optical fiber. The detector uses optical spectrum analyzer (OSA).

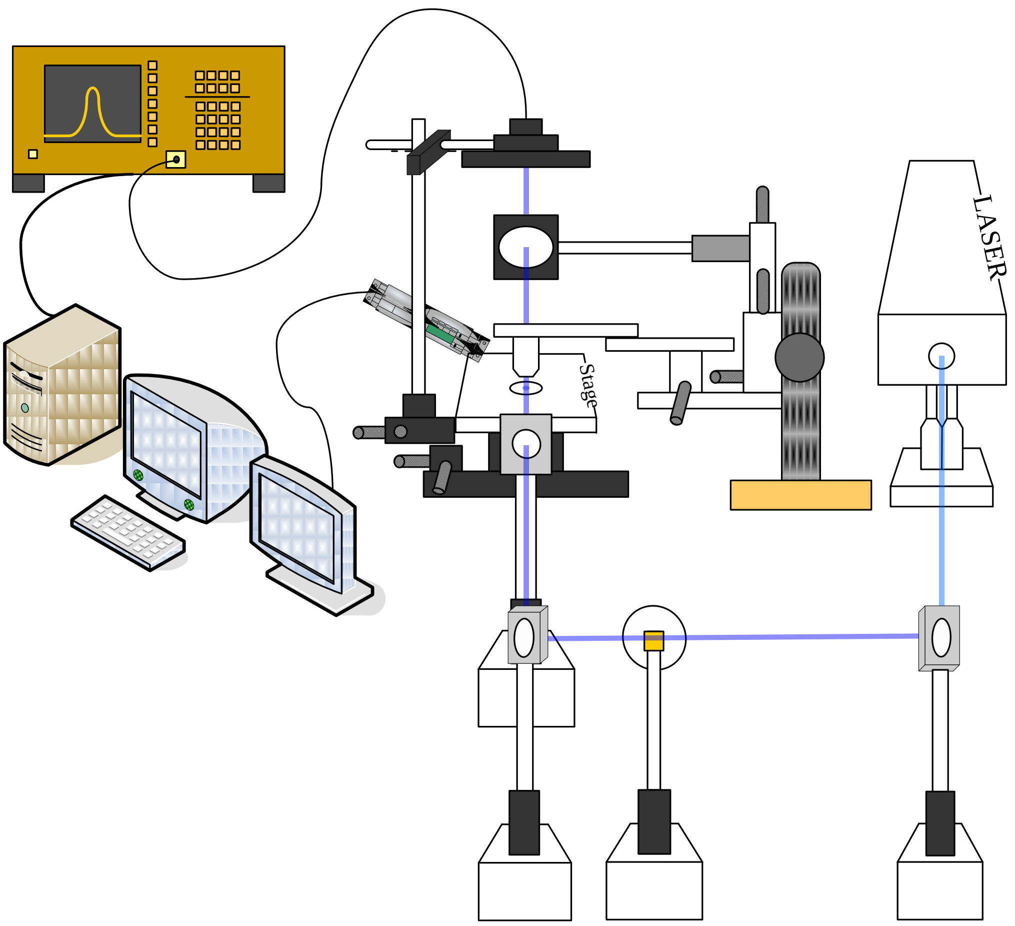

Fig. 2-6 The micro-photoluminescence system setup

2-4-4 Electroluminescence (EL)

Electroluminescence (EL) is an optical phenimenon and electrical phenomenon in which a LED emits light in response to an electric current passed through it, or to a strong electric field. EL is the result of radiative recimbination of electrons and holes in a LED. The excited electrons release their energy as photons. Prior to recombination, electrons and holes are separated either as a result of doping of the LED to form a p-n juction. The EL needs a LED device to inject excitation current, the device ready material property provides a chance for EL measurement directly on LED. The EL properties of LED are characterized through the EL spectrum, EL output power characteristics, and EL wavelength & EL full width at half maximum (FWHM) shift curves.

2-4-5 The Beam Profiler

Spatial characteristics describe the distribution of radiant energy across the wave front of an optical beam. The radiation can be shown as a plot of the relative intensity of points across a plane that intersects projected path of the beam.

We can use the beam profiler to observed the light intensity distribution of LED, then we know which structure or position can increase the light extraction.

2-4-6 The Radiation Pattern Measurement

As the scattering of light from the material itself to the external environment has a different refractive index, so the light scattering angle of light-emitting diode would be different because of their own material、the external environment and structural changes. The scattering angle measuring instrument structure as shown Fig. 2-7.

The light-emitting diodes placed on the stage, and the light intensity of LEDs at a 20 mA operation current were measured at the different angles through the stepper motor controller. Then, the detector used the optical spectrum analyzer (OSA), and connected to computer to analyze the data.

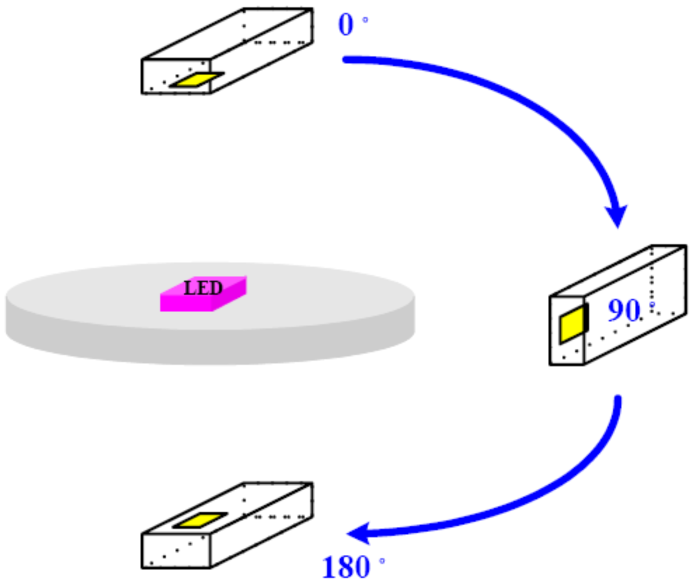

Fig. 2-7 The Radiation Pattern Measurement Instrument setup

Chapter 3 Results and Discussion

3-1 The Optical Microscopy (OM) of Light-Emitting Diode (LED)

The optical microscopy images of the ST-LED and the RPB-LED are shown in Fig. 3-1(a) and (b). After the crystallographic wet etching process, the treated grid lines that went across the LED chip were observed as a lightly-colored region that was caused by a high light-scattering phenomenon that occurred on the roughened patterned backside surface at the GaN/Al_2O_3 interface. The grid line width was measured at 20μm with a roughened backside surface. The GaN buffer layer acted as the sacrificial layer for the laser decomposition process and the lateral wet etching process with a 26μm/min etching rate.

The optical microscopy images of the patterned-sapphire LED (PS-LED) and the backside-roughened patterned-sapphire LED (BRPS-LED) after laser scribing process without wet etching are observed in Fig.3 -2(a) and (b). The optical microscopy images of the BRPS-LED after hot KOH etching are shown in Fig. 3-2(c). After the crystallographic wet etching process, the treated grid lines that were observed as a lightly-colored region that was caused by a high light-scattering phenomenon that occurred on the roughened patterned backside surface at the GaN/Al_2O_3 interface. The grid line width was measured at 18μm with a roughened backside surface on pattern sapphire substrate and the grid line gap was measured at 12.5μm.

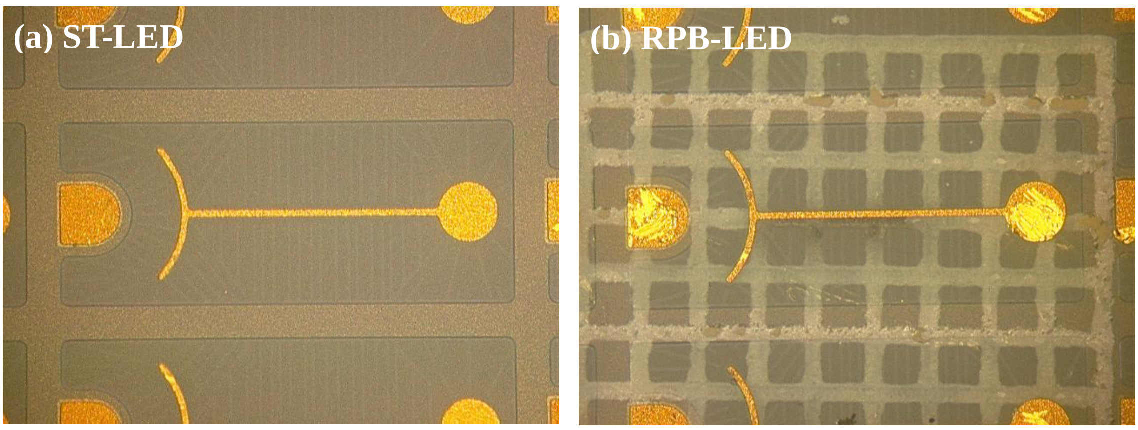

Fig. 3-1 The optical microscopy images of the (a) ST-LED and (b) RPB-LED

(a) PS-LED

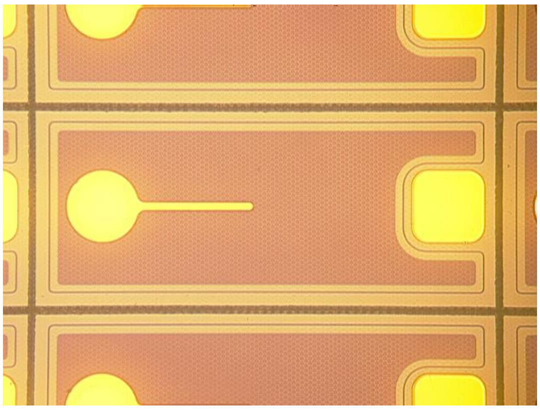

(b) BRPS-LED without wet etching

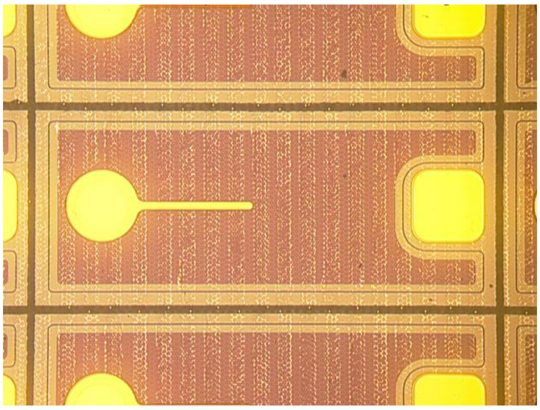

(c) BRPS-LED with wet etching

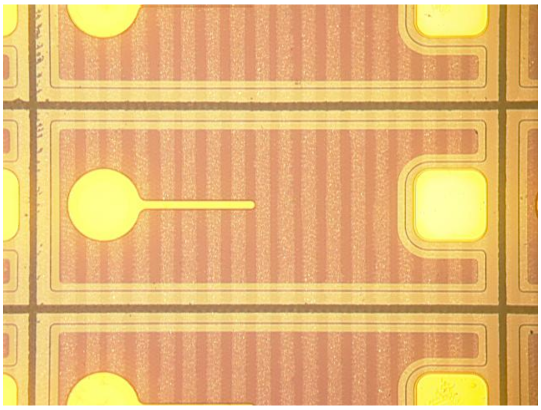

Fig. 3-2 The optical microscopy images of the (a) PS-LED, (b) BRPS-LED without wet etching and (c) BRPS-LED with wet etching.

3-2 The Cold Field Emission Scanning Electron microscopy (FE-SEM) of Light-Emitting Diode (LED)

From the cross-section SEM micrographs shown in Fig. 3-3(a)、(b)、(c) and (d), the inverted pyramidal-shaped structures were observed at the laser decomposition grid line after the crystallographic wet etching process. Fig. 3-3(a) and (b) were applied on flat-sapphire substrate, and Fig. 3-3(c) and (d) were applied on pattern-sapphire substrate. The GaN buffer layer decomposed as Ga metal and N_2 gas through the laser decomposition process. After the laser scribing process at the chip cutting line that provided the wet etching channel, the laser decomposition line was etched as a grid channel structure and a roughened N-face GaN surface was achieved through the crystallographic wet etching process in a hot KOH solution. The inverted pyramidal structure didn't have any contact with the bottom sapphire substrate at the grid line channel region of the roughened patterned backside on the N-face GaN surface at the GaN/Al_2O_3 interface. The $\{10\overline{1}1\}$ face group of the GaN layer has the most stable lattice planes with the lowest surface energy[16,17], anisotropic etching occurs with a continuous consumption of the $(000\overline{1})$ N-face and the gradual exposure of the non-etched stable $\{10\overline{1}1\}$ terminal faces of the GaN layer.

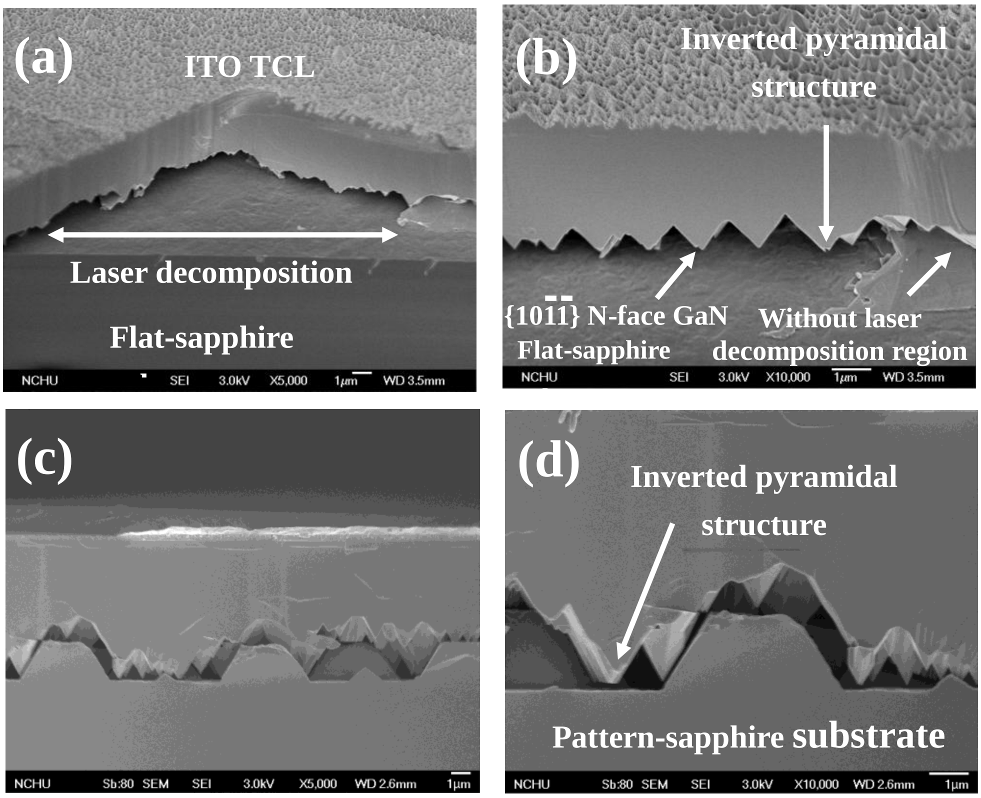

Fig. 3-3 The cross-section SEM micrographs of the RPB-LED are observed at 45° tilted angle, (a) without wet etching、(b) with wet etching and the BRPS-LED are observed at 90° tilted angle, (c) 5000X、(d)10000X.

3-3 The Intensity Distribution Graph of Light-Emitting Diode (LED)

The light-intensity profiles of both sapphire substrate-LED samples at a 20mA operation current were measured by a beam profiler shown in Fig. 3-4(a)、(b)、(c)、(d)、(e) and (f). In both-sapphire substrate, the light intensity of ST-LED and PS-LED were distributed uniformly on the whole LED mesa region. In both LED structures, the light intensity was almost the same in the mesa regions on the ITO layer without the backside crystallographic wet etching process. In the RPB-LED and BRPS-LED structure, a higher light-intensity was observed at the grid line regions, and at the gridline regions, a larger light-scattering process occurred on the roughened patterned backside N-face GaN surface. In Fig. 3-4(e) and (f), the light-scattering contributes not only occur on grid line but also on the pattern sapphire substrate. To analyze the light-intensity distribution over the entire LED chip, the line-scanning light-intensity profiles of both LED samples are shown in Fig. 3-4(g) where the observation positions are marked in Fig. 3-4(a)、(b) and shown in Fig. 3-4(h) where the observation positions are marked in Fig. 3-4(e)、(f) with dash lines along the x-axis. The resolution of the beam profiler is 0.35μm/pixel, where the mesa width of the LED image is 533μm.

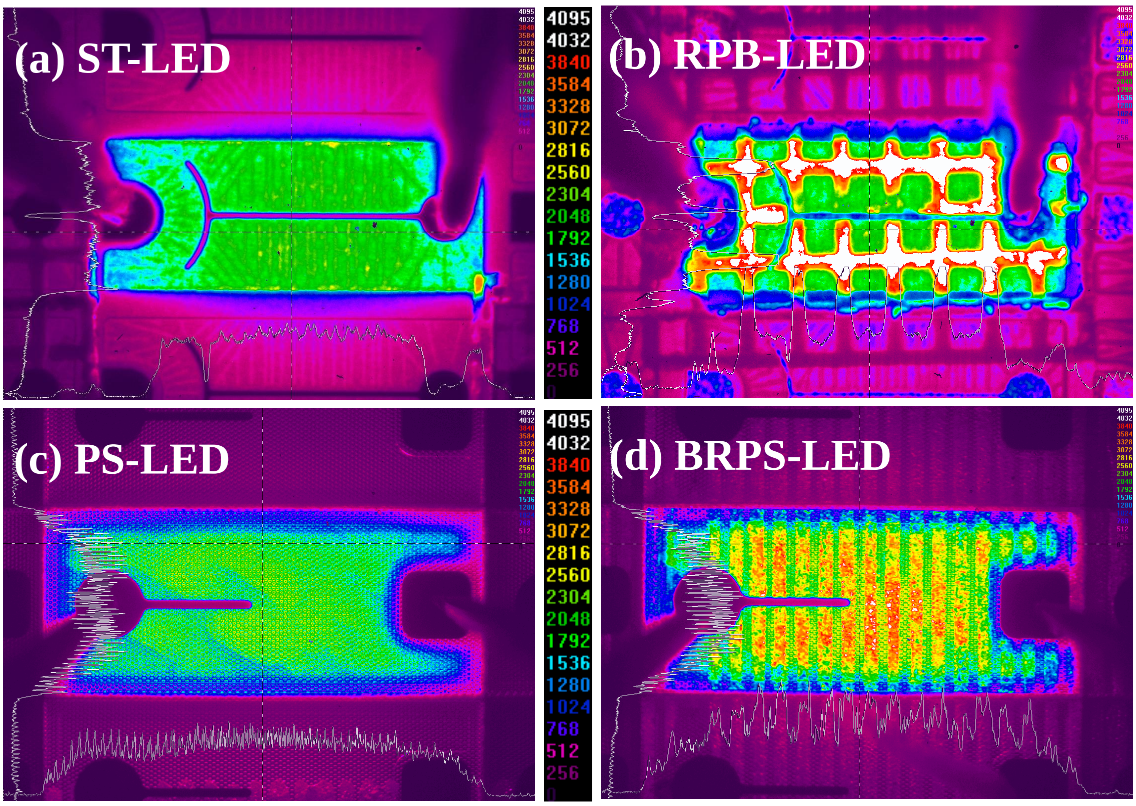

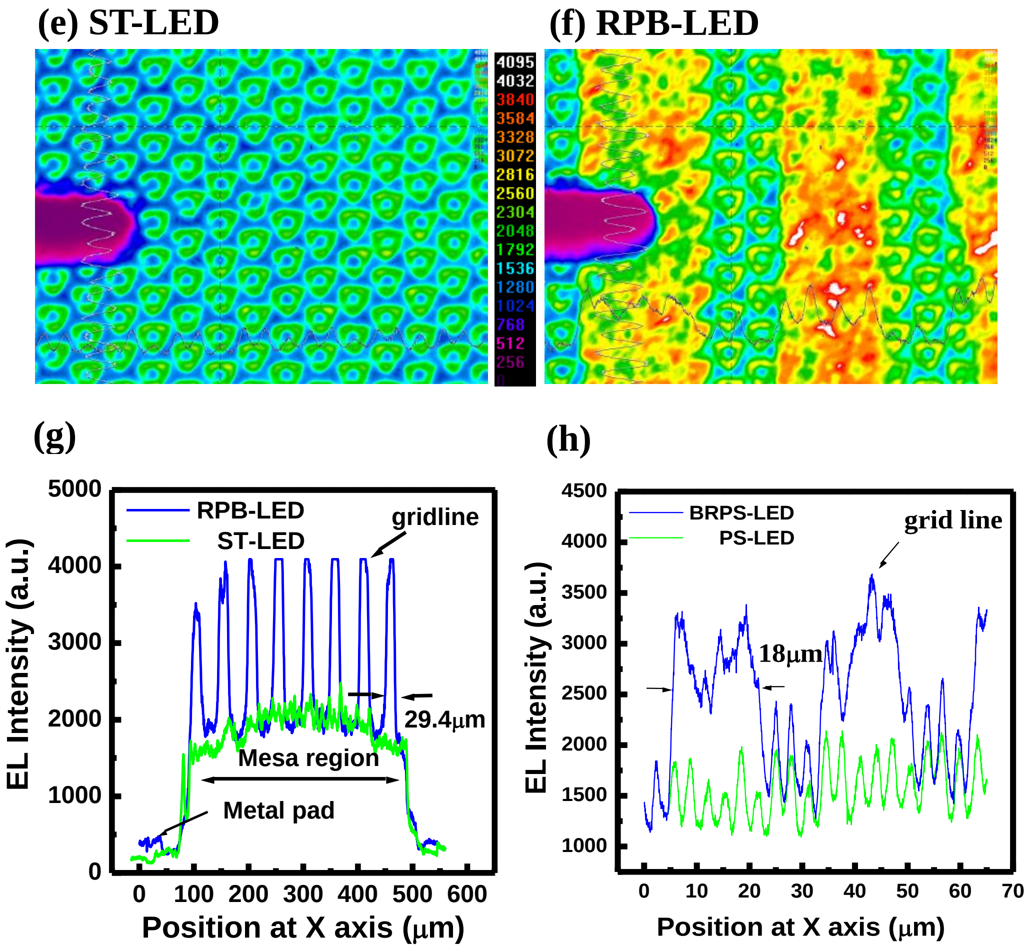

Fig. 3-4 The light-intensity profiles with 10X of (a) the ST-LED、(b) the RPB-LED、(c) the PS-LED and (d) the BRPS-LED at 20mA operation current are measured by a beam profiler. (e) and (f) are PS-LED and BRPS-LED with 100X. (g) and (h) The line-scan light intensities of LED structure with and without a roughened backside surface are measured here.

3-4 The Micro-Photoluminescence Spectroscopy (μ-PL) Measure of the Standard LED (ST-LED) and Roughened Patterned Backside Light-Emitting Diode (RPB-LED)

In Fig. 3-5, the peak wavelength and the relative emission-intensity of the μ-PL spectra were measured at 458.6nm (84.6 nW), 457.6nm (63.5 nW), and 460.6nm (46.2 nW) for the RPB-LED with the roughened patterned backside surface, the RPB-LED without the roughened patterned backside surface, and the ST-LED, respectively. The PL emission-light generated from the InGaN active layer propagated and scattered across the top surface, the bottom surface, and the mesa sidewall making it possible to analyze the light-extraction efficiency. [18] The PL intensity of the RPB-LED structure has a 1.83 times (with roughened backside surface) and a 1.37 times (without roughened backside surface) enhancement compared to the ST-LED structure where both LED samples had a backside-polished sapphire substrate. When the laser was focused on the mesa region (with roughened backside surface) of the RPB-LED structure, higher emission intensities of PL spectra were observed which could have been caused by the larger light scattering surface area and the higher light-extraction on the backside $\{10\bar{1}\bar{1}\}$ N-face planes fabricated through the laser decomposition process and the crystallographic wet etching process.

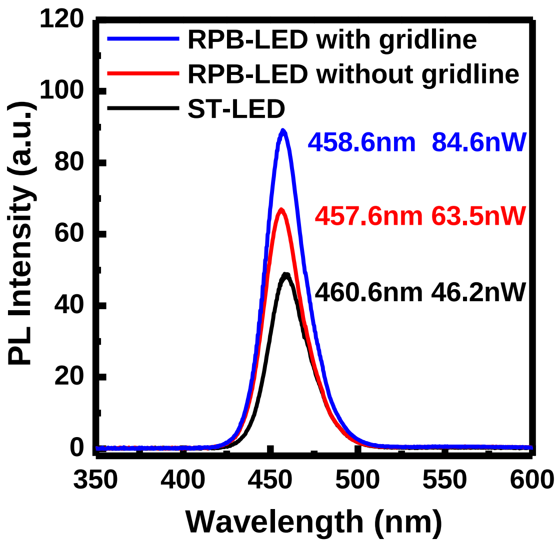

Fig. 3-5 When the laser spots focus on the RPB-LED with and without the roughened backside surface and on the ST-LED, theμ-PL spectra are measured at room temperature.

3-5 The Electroluminescence (EL) Emission Spectroscopy Measure of the Standard LED (ST-LED) and Roughened Patterned Backside Light-Emitting Diode (RPB-LED) and The Electrical Properties Measure of Both Sapphire Light-Emitting Diode (LED)

In Fig. 3-6(a), the peak wavelength of the EL spectrum was measured at about 453nm for both LED structures at a 20mA operating current, and the higher EL emission intensity of the RPB-LED compared to the ST-LED was also measured. In Fig. 3-6(b) and (c), the light-output power and the operating voltage as functions of the DC injection current were measured, and the light-output power of the RPB-LED had a 47% enhancement compared to the ST-LED and the BRPS-LED had a 21.4% enhancement compared with the PS-LED at a 20mA operating current. In Fig. 3-6(b), the operating voltages of both LED samples were almost the same, at the value of 3.18V at 20mA, and in Fig. 3-6(d) is shown the value of 3.42V at 20mA, because the treated grid line regions were located at the bottom of the LED structure close to the sapphire substrate without any effect on the active layer. The higher light-output power of the RPB-LED was caused by the higher scattering process from the bottom pyramidal roughened surface that increased external quantum efficiency.

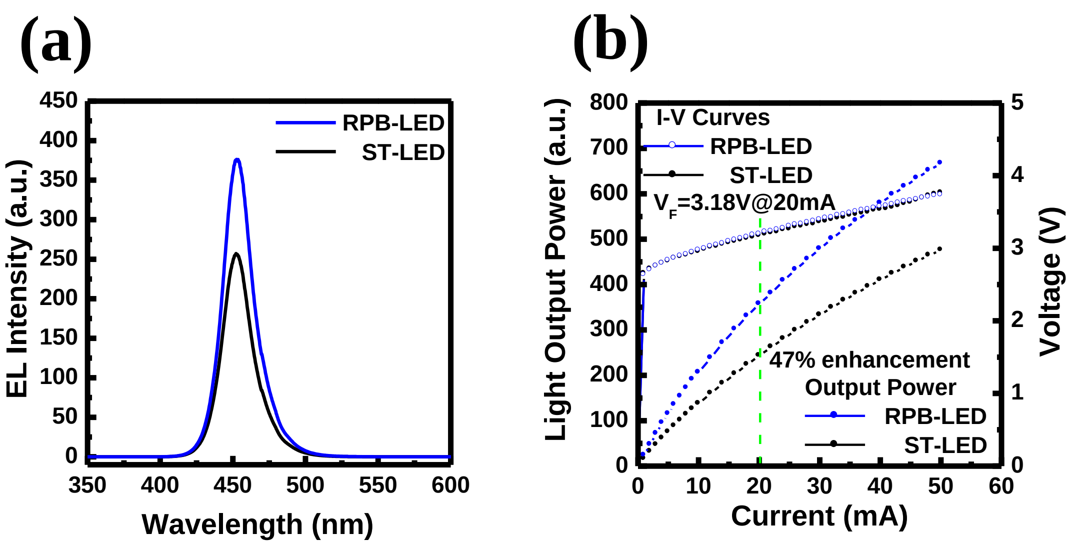

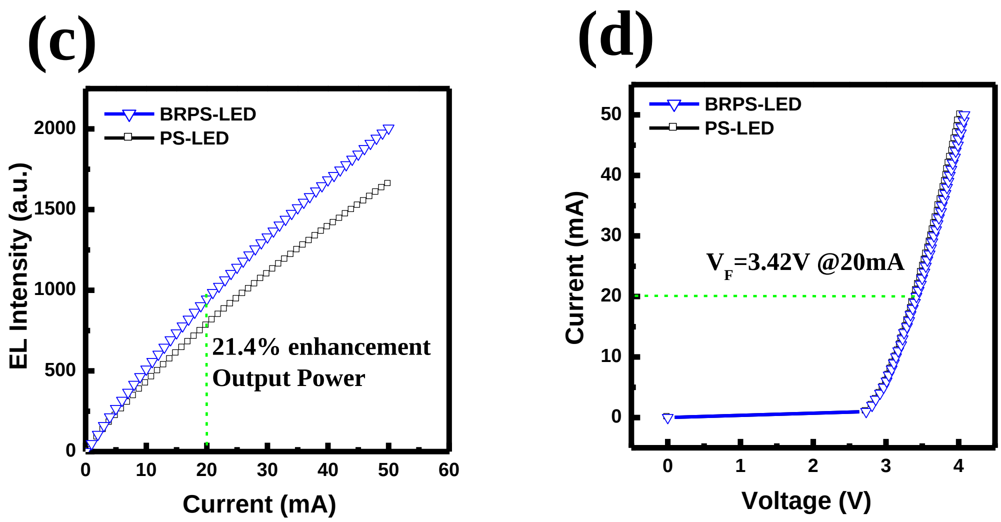

Fig. 3-6 (a) The EL emission wavelength is measured at about 453nm for both LED structures at a 20mA operating current. (b) For flat-sapphire LED samples, the current-voltage characteristics and the light-output power, and for pattern-sapphire LED samples, (c) the light-output power and (d) the current-voltage characteristics as a function of the operating current are measured here.

3-6 The Radiation Pattern Measure of Both Sapphire Light-Emitting Diode(LED)

At 20mA, the far-field radiation patterns and the light-enhanced ratios of both-sapphire LED samples were measured from normal direction to the back-side direction as shown in Fig. 3-7(a) (a)、(b)、(c) and (d). The detection angle (θ) from the LEDs top surface is defined as 90°. For flat-sapphire LED, the divergent angles measured on the top side (θ: 0°-180°) of the ST-LED and the RPB-LED were calculated at values of 157° and 137°. For pattern-sapphire LED, the divergent angles of the PS-LED and the BRPS-LED were calculated at values of 112° and 119°, respectively. The smaller divergent angle of RPB-LED is induced by light-gathering at the axial and the larger divergent angle of BRPS-LED is induced by light-scattering process from the inverted pyramidal-shaped structures on the roughened patterned backside surface at the GaN/Al_2O_3 interface. The high light intensity at the normal direction of the PS-LED caused by the higher light scattering process on the triangle-shaped patterned sapphire structure. In the RPB-LED and BRPS-LED structure, the high light intensity was observed at the normal direction and the backside direction that was caused by the higher light scattering process on the inversed cone-shaped structure and the patterned sapphire substrate. The total light-enhanced ratio of the RPB-LED was 1.34 times higher compared to the ST-LED, and the BRPS-LED was 1.12 times higher compared to the PS-LED, respectively.

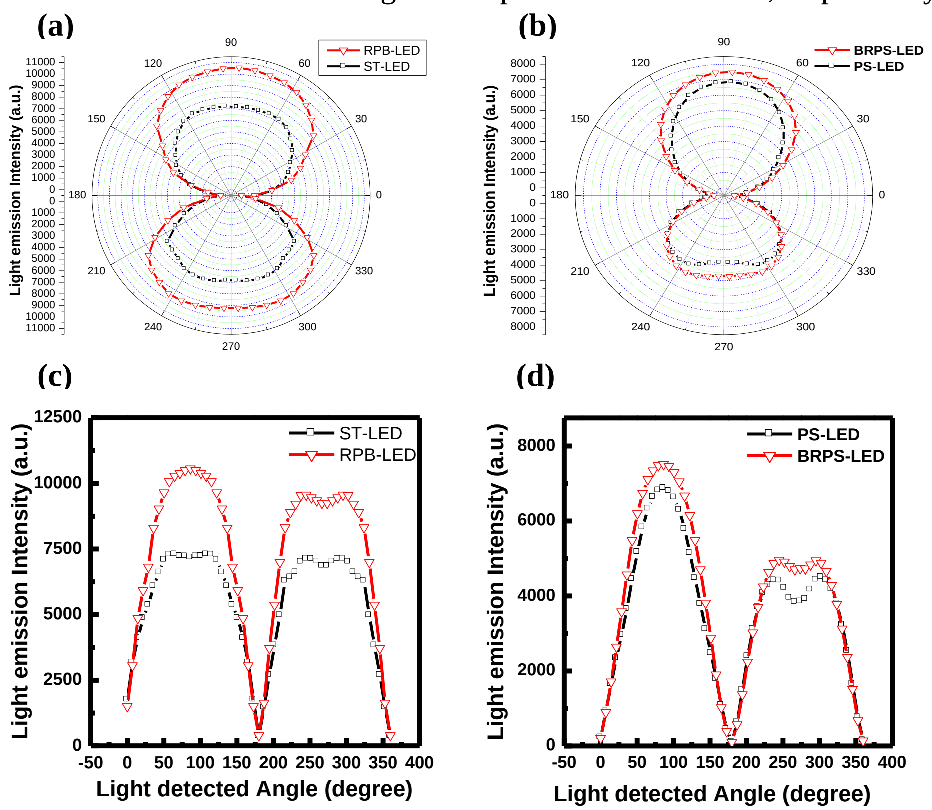

Fig. 3-7 LED show measurements of (a) and (b) far-field radiation patterns and (c) and (d) light-enhanced ratios from the normal direction to the back-side direction.

3-7 The Efficiency Measure of Pattern Sapphire Light-Emitting Diode(LED)

The RBPS-LED structure consisted of a truncated triangle-shaped patterned-sapphire substrate, a step-inverted pyramidal structure, and laser-scanning striped-line patterns to increase the light extraction efficiency. The high light scattering process occurred at the roughened N-face GaN surface and the GaN/air/patterned-sapphire interfaces. By increasing the pulse operation current up to 200mA (176 A/cm^2), the related efficiency droop property and the peak wavelength blueshift phenomenon were almost the same in both LED structures are shown in Fig. 3-8. The LEDs with the step-inverted pyramidal structure and the GaN/air-gap/patterned-sapphire interfaces had high light-extraction efficiency for the nitride-based LEDs without removed the sapphire substrates.

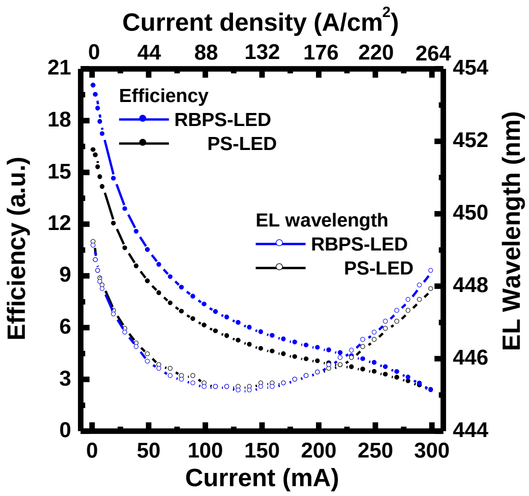

Fig. 3-8 The external quantum efficiency and the peak EL wavelength as the function of the pulse operating current were measured.

3-8 The Solar Cell Characteristics Measure of Flat Sapphire Light-Emitting Diode(LED)

3-8-1 The fabrication of the RB-LESC structure

Using a triple frequency ultraviolet Nd:YVO_4 (355nm) laser for the backside GaN melting and decomposition process. During the laser melting process at GaN buffer layer, the laser spot was focus on the bottom GaN/patterned-sapphire interface. The striped-line patterns, with a 20μm-width by varying spacing widths, were fabricated through a backside laser melting process on GaN buffer layer at the GaN/sapphire interface. The LED structures with the striped-line spacing varied from 40μm, 30μm, 20μm and 10μm at the mesa region were defined as the roughened-backside with 40μm-spacing LED (RB40-LED), RB30-LED, RB20-LED, and RB10-LED, respectively. The GaN buffer layer decomposed as Ga metal and N_2 gas through the laser decomposition process. The LED wafer was immersed in a hot KOH solution (KOH, 80°C) for a 15-minute lateral crystallographic wet etching process that occurred at the laser treated striped-line pattern regions. The wet etching process consisted of a selective lateral etching process on a GaN buffer layer and a bottom-up N-face crystallographic etching process to form the pyramidal N-face GaN structure close to the GaN/sapphire interface. The LED device that was fabricated through this process flow without a laser decomposed process was defined as a standard LED (ST-LED). The chosen ST-LED and RB-LED were both located at the 2" LED wafer center to allow for analysis of the optical and electrical properties in more similar material properties. The schematic of the roughened backside Light-Emitting Solar Cell (RB-LESC) structure and the process steps are shown in Fig. 3-9.

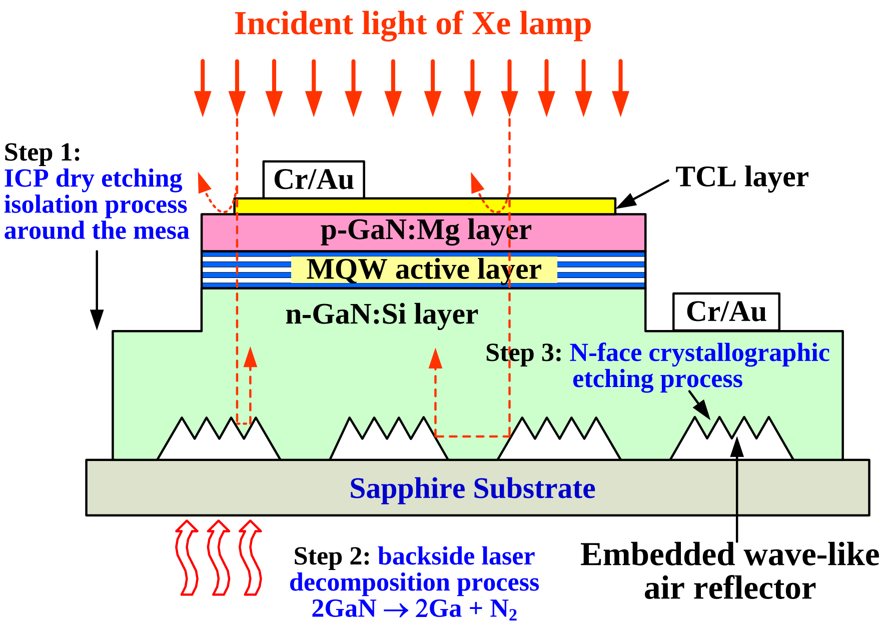

Fig. 3-9 The schematic of the RB-LESC structure

3-8-2 The Intensity Distribution Graph of Light-Emitting Diode (LED)

In Fig. 3-10, the light-intensity profiles of the RB-LESC structures at a 20mA operation current were measured by a beam profiler. The spacing width of each stripe-line structures was varied from 40μm, 30μm, 20μm, and 10μm for the RB40-LESC, RB30-LESC, RB20-LESC, and RB10-LESC, respectively. In the RB-LED structure, a higher light-intensity was observed at the stripe-line regions that had larger light-scattering process occurred on the roughened backside N-face GaN surface. The light emission intensity on the strip-line region is higher than on the region without laser scanning process, and the light intensity of each stripe-line patterns are almost all the same.

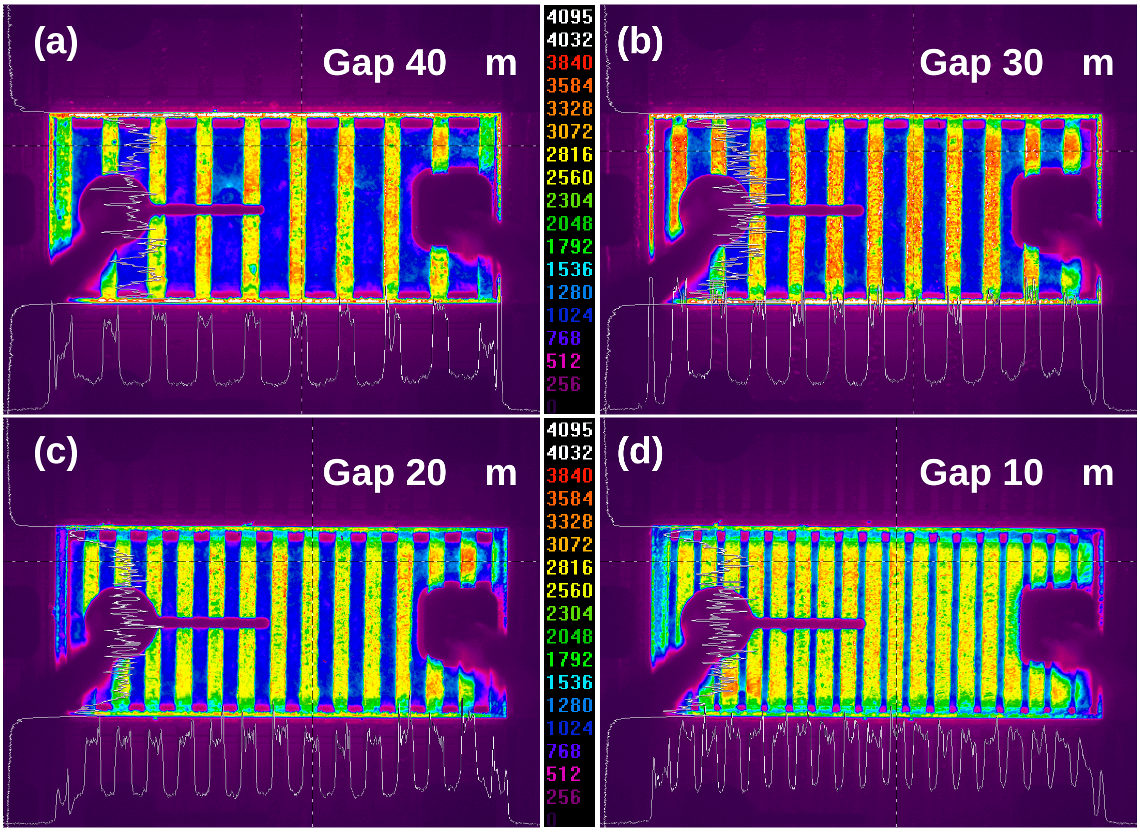

Fig. 3-10 The light-intensity profiles of (a) RB40-LESC, (b) RB30-LESC, (c) RB20-LESC, and (d) RB10-LESC at 20mA operation current are measured by a beam profiler, respectively.

3-8-3 The Photovoltaic Characteristics of Light-Emitting Diode (LED)

Fig. 3-11(a) shows the current density-voltage (J-V) characteristics of the ST-LESC and the RB-LESCs measured under the illumination of air mass (AM) 1.5G condition. The open-circuit voltage (Voc), short-circuit current density (Jsc) of all LESC structures were also measured. All the LESCs structures had the same Voc values of 2.3 V. The Jsc value of the ST-LESC was measured at 0.61 mA/cm^2. By reducing the spacing-width from 40μm to 10μm, the Jsc value of the RB-LESC structures were increased from 0.83mA/cm^2 to 1.23 mA/cm^2 by increasing the backside roughened area at the mesa region. The external quantum efficiency (EQE) as a function of the illuminated wavelength was shown in Fig. 3-11(b). The peak EQE values were measured at 0.42 (at 371.4 nm), 0.54 (at 372.5 nm), 0.64 (at 373.0 nm), 0.70 (at 373.1nm), and 0.75 (at 373.4 nm) for the ST-LESC, RB40-LESC, RB30-LESC, RB20-LESC, and RB10-LESC, respectively. The peak wavelength of the EQE spectra of the BR-LESC structures had a slightly redshift phenomenon by increasing the backside roughened area ratio on the mesa region. The peak EQE value and short-circuit current density were measured as a function of the backside roughened area ratio shown in Fig. 3-11(c). The peak EQE value and Jsc were increased by increasing the laser-treated roughened area ratio. The highest peak EQE value and Jsc were measured at 0.75 (at 373.4 nm) and 1.23mA/cm^2 for the RB-LESC structure.

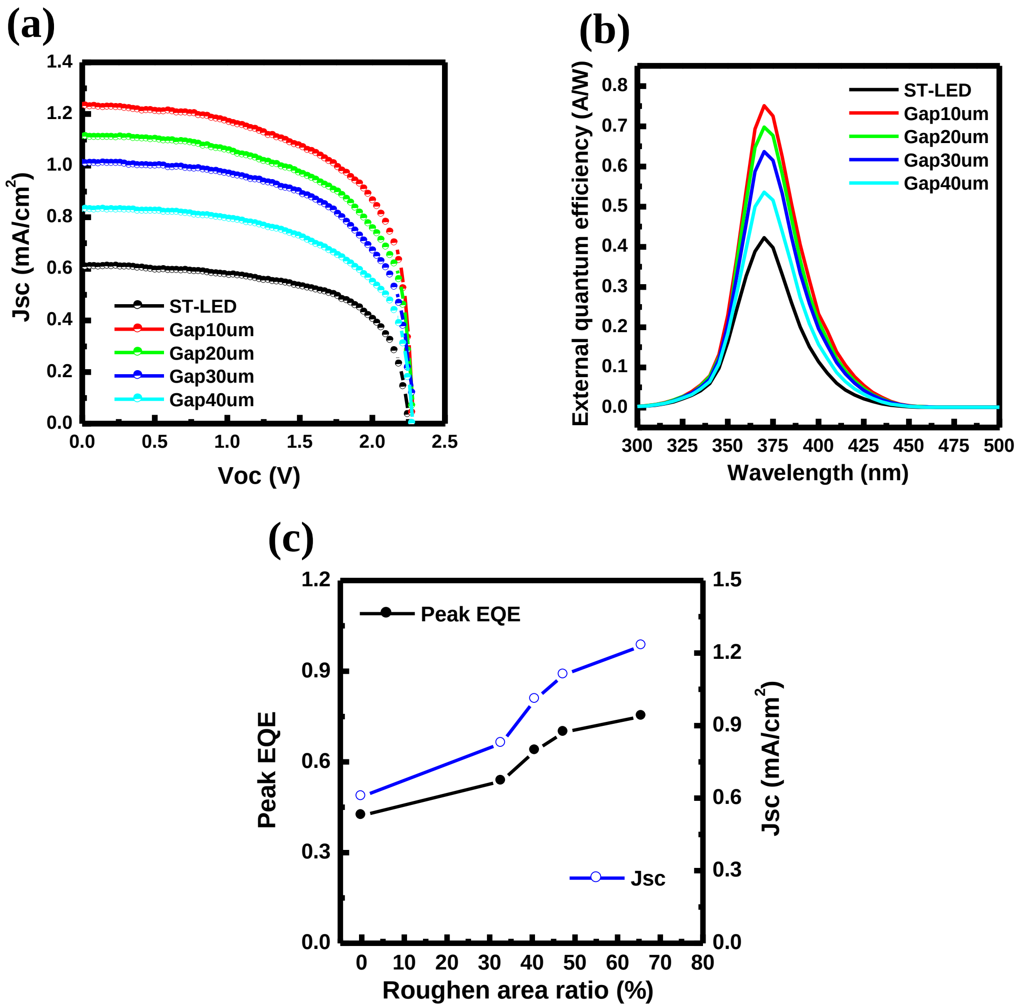

Fig. 3-11 (a) shows the current density-voltage (J-V) characteristics of the ST-LESC and the RB-LESCs. (b) The external quantum efficiency (EQE) as a function of the illuminated wavelength. (c) The peak EQE value and short-circuit current density were measured as a function of the backside roughened area ratio.

Reference

[1] S. Nakamura and G. Fasol, 1997. The Blue Laser Diode. New York:Springer.

[2] M. A. Khan, J. N. Kuznia, A. R. Bhattarai, and D. T. Olson, 1993. Metal semiconductor field effect transistor based on single crystal GaN, Appl. Phys. Lett., 62, 1786–1787.

[3] E. S. Fred, 2003 . Light-Emitting Diodes, Cambridge, U.K.: Cambridge Univ.Press.

[4] R. J. Xie, N. Hirosaki, M. Mitomo, K. Takahashi, and K. Sakuma, 2006. Highly efficient white-light-emitting diodes fabricated with short-wavelength yellow oxynitride phosphors, Appl. Phys. Lett., 88, 101104.

[5] K. Tadatomo, H. Okagawa, Y. Ohuchi, T. Tsunekawa, Y. Imada, M. Kato, and T. Taguchi, 2001. High output power InGaN ultraviolet light-emitting diodes fabricated on patterned substrates using metalorganic vapor phase epitaxy, Jpn. J. Appl. Phys., 40, 583.

[6] C. Huh, K. S. Lee, E. J. Kang, and S. J. Park, 2003. Improved light-output and electrical performance of InGaN-based light-emitting diode by microroughening of the p-GaN surface, J. Appl. Phys., 93, 9383.

[7] S. J. Chang, L. W. Wu, Y. K. Su, Y. P. Hsu, W. C. Lai, J. M. Tsai, J. K. Sheu, and C. T. Lee, 2004. Nitride-based LEDs with 800℃ grown p-AlInGaN-GaN double-cap layers, IEEE Photon. Technol. Lett., 16, 1447.

[8] A. David, T. Fujii, R. Sharma, K. Mcgroody, S. Nakamura, S. P. DenBaars, E. L. Hu, and C. Weisbuch, 2006. Photonic-crystal GaN light-emitting diodes with tailored guided modes distribution, Appl. Phys. Lett., 88, 061124.

[9] H. K. Cho, J. Jang, J. H. Choi, J. Choi, J. Kim, J. S. Lee, B. Lee, Y. H. Choe, K. D. Lee, S. H. Kim, K. Lee, S. K. Kim, and Y. H. Lee, 2006. Light extraction enhancement from nano-imprinted photonic crystal GaN-based blue light-emitting diodes, Optics Express, 14, 8654-8660.

[10] H. G. Kim, M. G. Na, H. K. Kim, H. Y. Kim, J. H. Ryu, T. V. Cuong, and C. H. Hong, 2007. Effect of periodic deflector embedded in InGaN/GaN light emitting diode, Appl.Phys. Lett., 90, 261117.

[11] C. F Lin, Z. J. Yang, J. H. Zheng, and J. J. Dai, 2005. Enhanced light output in nitride-based light-emitting diodes by roughening the mesa sidewall, IEEE Photon. Technol. Lett., 17, 2038.

[12] T. Fujii, Y. Gao, R. Sharma, E. L. Hu, S. P. DenBaars, and S. Nakamura, 2004.

Increase in the extraction efficiency of GaN-based light-emitting diodes via surface roughening, Appl. Phys. Lett., 84, 855.

[13] H. G. Kim, T. V. Cuong, M. G. Na, H. K. Kim, H. Y. Kim, J. H. Ryu, and C. H. Hong, 2008. Improved GaN-Based LED Light Extraction Efficiencies via Selective MOCVD Using Peripheral Microhole Arrays, IEEE Photon. Technol. Lett., 20, 1284.

[14] D. A. Stocker, E. F. Schubert, and J. M. Redwing, 1988. Crystallographic wet chemical etching of GaN, Appl. Phys. Lett., 73, 2654.

[15] S. Nakamura, M. Senoh, N. Iwasa, and S. Nagahama, 1955. High-brightness InGaN blue, green and yellow light-emitting diodes with quantum well structures, Jpn. J. Appl. Phys. Part 2, 34, 797.

[16] Y. Gao, M. D. Craven, J. S. Speck, S. P. DenBaars, and E. L. Hu, 2004. Dislocation- and crystallographic-dependent photoelectrochemical wet etching of gallium nitride, Appl. Phys. Lett., 84, 3322.

[17] H. M. Ng, N. G. Weimann, and A. Chowdhury, 2003. GaN nanotip pyramids formed by anisotropic etching, J. Appl. Phys., 94, 650.

[18] J.S. Lee, J. Lee, S. Kim, and H. Jeon, 2006. GaN-based light-emitting diode structure with monolithically integrated sidewall deflectors for enhanced surface emission, IEEE Photon. Technol. Lett., 18, 1588.